Check for updates

Research progress in the development of organic small molecule fluorescent probes for detecting H$_2$O$_2$

Yuanyuan Liu,[abcd] Chunpeng Jiao,[abcd] Wenjuan Lu,[bcd] Pingping Zhang[bcd] and Yanfeng Wang [ID] *[bcd]

Hydrogen peroxide (H$_2$O$_2$), as an important signaling molecule during biological metabolism, is a key member of the reactive oxygen species (ROS) family. The excess of H$_2$O$_2$ will lead to oxidative stress, which is a crucial factor in the production of various ROS-related diseases. In order to study the diverse biological roles of H$_2$O$_2$ in cells and animal tissues, many methods have been developed to detect H$_2$O$_2$. Recently, fluorescence imaging has attracted more and more attention because of its high sensitivity, simple operation, experimental feasibility, and real-time online monitoring. Based on the response group, this study will review the research progress on hydrogen peroxide and summarizes the mechanisms, actualities and prospects of fluorescent probes for H$_2$O$_2$.

1. Introduction

In the oxygen-containing metabolism process, the living organism produces a variety of free radicals and derivatives with redox activity,[1,2] and reactive oxygen species (ROS) are one of them. Reactive oxygen species includes superoxide (O$_2^-$), hydroxyl radical (·OH), hydrogen peroxide (H$_2$O$_2$), hypochlorous acid (HOCl) and so on, and their initial active substance is O$_2^-$. In living organisms, O$_2^-$ is the basis for the formation of other reactive oxygen species.[3,4] As is shown in Fig. 1, oxygen is catalyzed by NADPH (nicotinamide adenine dinucleotide phosphate) oxidase (NOX) to form O$_2^-$ *via* single electron reduction.[5,6] Subsequently, the two O$_2^-$ are capable of forming H$_2$O$_2$ under the action of superoxide dismutase (SOD).[7–9] H$_2$O$_2$ is converted to ·OH in the presence of a single electron metal ion such as Fe^{2+} undergoing Fenton reaction, and interacts with Cl$^-$ to form HOCl in the presence of myeloperoxidase (MPO).[10–12] As shown in the figure, when reacting with O$_2^-$, HOCl can convert into ·OH further.[5,13] Arginine reacts with various nitric oxide synthase (NOS) enzymes to produce nitric oxide (NO), which reacts with O$_2^-$ to produce peroxynitrite (ONOO$^-$).[14–17] Peroxynitrite can decompose to form hydroxyl radicals by interaction with hydrogen ions (H$^+$).

H$_2$O$_2$ in cells is mainly derived from mitochondria, endoplasmic reticulum (ER) and various oxidases.[18–21] Among the above sources, protein-type oxidase plays a critical role in generating H$_2$O$_2$ for signal conversion purposes. H$_2$O$_2$, one of the key members of the ROS family, has a certain regulatory effect on many physiological processes of organisms.[22,23] First, H$_2$O$_2$ is relevant to cell migration, proliferation and differentiation. Second, H$_2$O$_2$ has an immense influence on angiogenesis and vascular diameter regulation. Third, H$_2$O$_2$ can reversibly oxidize the proteins involved in the reaction, thereby activating or deactivating the pathway. In addition, it can effectively regulate the body's immune defence mechanism. For example, NADPH in neutrophils produces μM-grade H$_2$O$_2$ to kill pathogens.[24] Finally, H$_2$O$_2$ is closely connected with oxidative stress-associated cancers. In the case of oxidative stress, the concentration of H$_2$O$_2$ will increase to 10–15 μM, which will further aggravate the condition of vasodilation cancer.[25]

[a]School of Medicine and Life Sciences, University of Jinan-Shandong Academy of Medical Sciences, Jinan 250200, Shandong, China

[b]Institute of MateriaMedica, Shandong Academy of Medical Sciences, Jinan 250062, Shandong, China. E-mail: wyfshiwoya@126.com

[c]Key Laboratory for Biotech-Drugs Ministry of Health, Jinan 250062, Shandong, China

[d]Key Laboratory for Rare & Uncommon Diseases of Shandong Province, Jinan 250062, Shandong, China

Fig. 1 The interaction between H$_2$O$_2$ and other ROS.

As a vital signal molecule in the process of biological metabolism, hydrogen peroxide is attracting more and more attention for its ideal signal characteristics. First, it has adequate chemical reactivity to react with potential signal targets, and has sufficient stability to diffuse within the cell for a certain distance to react with the target selectively.[26] Moreover, it can be generated rapidly, diffused and eliminated quickly, which makes it suitable as a signal generating substance. Normally, the average concentration of H_2O_2 in healthy mammalian cells ranges from 1 to 700 nM, and this low concentration of homeostasis is beneficial for normal cell growth. High concentrations of H_2O_2 can contribute to oxidative stress in the biological system and trigger apoptosis.[27] Excessive accumulation of hydrogen peroxide in the human body can cause a series of inflammations and diseases, such as cancers,[28] Alzheimer's disease[29] and cardiovascular diseases[30] and also affects early embryological development in mammals. H_2O_2 is mainly used as a bleaching agent and disinfectant in life and plays an irreplaceable and indispensable role in the living system.

At present, studying the dynamic distribution of H_2O_2 in living cells and monitoring the concentration change of H_2O_2 in the human body are going to become a pivotal focus for biology. As an important tool, fluorescent probes have become a research hotspot in life sciences because it can greatly reduce the detection limit and has strong sensitivity and selectivity. As Scheme 1 shows, the binding of H_2O_2 to response group can lead to either enhancement (turn-on), quenching (turn-off) or ratio change of the fluorescence intensity, coupled with a red or blue shift of the emission band or absorption band. Here selective fluorescent probes are used for monitoring H_2O_2. In order to gain a better analysis on how H_2O_2 is generated in living systems as well as to illustrate its biological roles.

In 1965, Richard Brandt and Albert Keston designed a stable reagent probe **1** (Fig. 2) to detect H_2O_2, inspired by Schales.[31,32] In the presence of H_2O_2, nonfluorescent compound **1** can rapidly oxidized to a fluorescent compound. Shortly after publication of this paper, Stephen Hempel and Duane Wessels used probe **1** as a detector of intracellular oxidants.[33] Their work demonstrated that probe **1** was a better fluorescent probe for detecting intracellular oxidants such as hydroxyl radical and
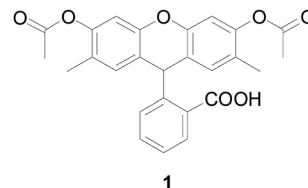

Fig. 2　Structure of probe **1**.

nitric oxide because it is more reactive toward specific oxidizing species.

With the development of technology, fluorescence analysis is becoming maturer and maturer. Thus, the number of fluorescent probes for detecting H_2O_2 is increasing gradually. The application of fluorescent probe to expound biological events relate to H_2O_2 has significantly promote the progress of H_2O_2-probes in the field of medicine and biology. In this review, five types of H_2O_2-specific fluorescent probes in probes treasury will mainly summarized and introduced based on their response group, including arylboronate-based probes, sulfonate-based probes, benzoyl-based probes, o-benzenediol based probes and enamine-based probes. These probes can not only largely improve selectivity and sensitivity to H_2O_2, but are also widely used as agents for bioimaging of H_2O_2. In addition, this review will discuss the molecular mechanism, current situation and prospects of H_2O_2 fluorescent probes.

2.　Arylboronate-based fluorescent H_2O_2 probes

Conventional H_2O_2 fluorescent probes often comprise a H_2O_2-sensing moiety, a fluorophore and a linker. The most commonly used response moiety for H_2O_2 is arylboronate, which has developed in many fluorophores to monitor H_2O_2 in living cells and tissues. As early as 1957, Henry and Albert[34] studied the response mechanism of hydrogen peroxide to arylboronic acids in aqueous solutions (Fig. 3). The nucleophilic H_2O_2 attacks the electrophilic aryl borate to form an unstable intermediate, which was hydrolyzed to produce phenol and boric acid quantitatively.

In 2003, Lo and co-workers[35] first developed probe **2a** and **2b** (Fig. 4), whose skeleton consisted of the same response site and
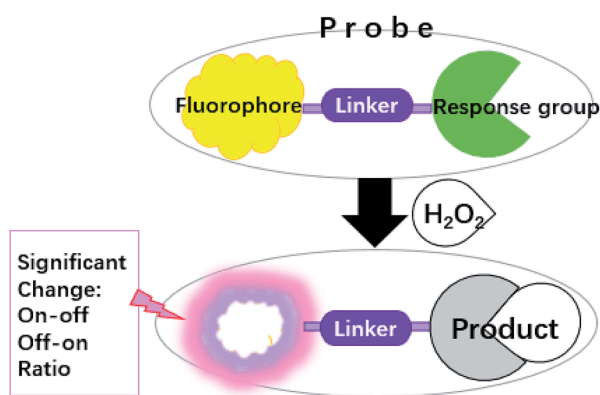
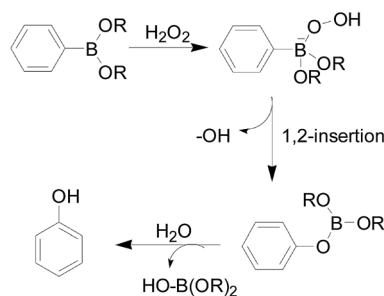Scheme 1　Design of the fluorescence molecular probes for H_2O_2 detection.

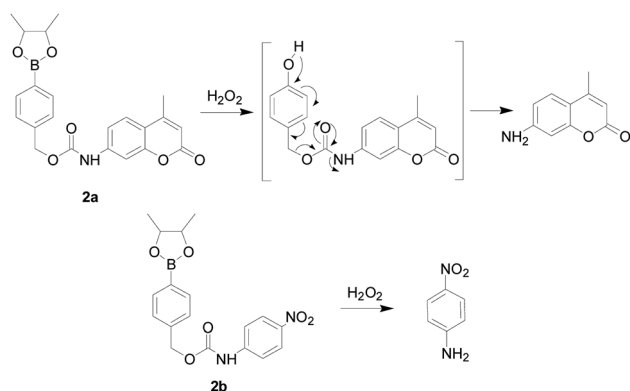Fig. 3　Mechanism of fluorescent probes based on arylboronate functionality to H_2O_2.

Fig. 4 Sensing mechanism of probe **2a** and **2b** by H_2O_2.

the different amino group as suitable reporter groups. Both of these stable probes could be activated upon reaction with H_2O_2 and released the corresponding sensing group. A good linear reaction between the released p-nitroaniline or coumarin group and the hydrogen peroxide in the solution. The difference was that probe **2a** provided a more sensitive detection range (0.1 to 5 mM) than probe **2b**. Carried different special properties reporter groups could not affect the detecting mechanism was the major advantages in the design of the probes in this article, which could be used to meet the demands. However, the response time of both probes was much longer. Therefore, these probes have not been used in cell imaging experiments.

In 2004, Chang's group[36] reported a H_2O_2 probe **3** (Fig. 5), they first introduced a pinacol borate into a fluorescent probe. It was a new water-soluble, turn-on optical probe, containing two boronic ester groups at the 3′ and 6′ positions of a xanthenone scaffold as a response moiety. It is worth mentioning that probe **3** had a high selectivity and sensitivity, exhibiting a >500-fold higher response for H_2O_2 over other similar ROS such as ·OH or

Fig. 5 Fluorescence response of **3** to H_2O_2 and the structure of **4** and **5**.

OCl^-. The authors believe this is because the reaction is a deprotection process rather than an oxidation reaction. Furthermore, the probe was applied to fluorescence imaging of exogenous H_2O_2 in human embryonic kidney cells (HEK293T cells) and good results were obtained. Subsequently, this research group[37–40] designed a series of probes based on this mechanism. The commonality of these probes were fluorescein used as a fluorophore, an aryl boronate used as a response site, and structural modification performed there on. In the same year, Zhao and colleagues[41] designed a dual-response fluorescent-opening probe **4** (Fig. 5), which connected the PF1-derivative to the coumarin unit via a disulfide bond, and simultaneously responds to H_2O_2 and bio-thiols. The team evaluated the selectivity and sensitivity of the probe and found that probe **4** showed a positive response to H_2O_2 and thiol-containing DL-dithiothreitol (DTT), glutathione (GSH), homocysteine (Hcy), and cysteine (Cys) only. Furthermore, H_2O_2 exhibited a different response than DTT, GSH, Hcy and Cys. When the probe was treated with H_2O_2, the di-borate group converted to a hydroxyl to form a highly fluorescent fluorescein derivative, and the original PET process converted to an intra-molecular FRET mechanism to cause the fluorescence to turn on. Probe **4** could be activated by endogenous thiol and exogenous H_2O_2, and thus had the applicability to both inside and outside the cell. However, the response time and detection limit were not satisfactory. In 2017, Hailei Zhang's team[42] modified the nanoparticle HNTs with fluorescein derivative PA to prepare probe **5** (PA-HNTs), which has a highly specific fluorescent "turn-on" response to H_2O_2. Nanocomposites exhibit regular morphology and good dispersibility in aqueous solution (Fig. 5). Experiments showed that **5** can monitor H_2O_2 produced by A549 cells under physiological conditions, which provided a good tool for tumor diagnosis. In order to track H_2O_2 at a low level to prevent and diagnose related diseases, it was necessary to develop a H_2O_2 sensitive fluorescent probe.

The group headed by Binghe Wang[43] reported a simple fluorescent probe that directly binds the borate ester group to coumarin. This probe showed 100-fold increase in fluorescent intensity upon reaction with H_2O_2 and showed selectivity over other ROS, but the probe had a short emission wavelength at 454 nm. Subsequently, the research group[44] improved this conjugate system by introducing a triazole into the molecule to obtain a new probe **6** (Fig. 6). Its emission wavelength was red shifted to 474 nm, and its selectivity to H_2O_2 was 2–4 times higher than that of other ROS, which was more suitable for cell and in vivo imaging. But the disadvantage was that the fluorescent intensity only increased 5-fold. In the above reports, borate ester group could be used as the response site of
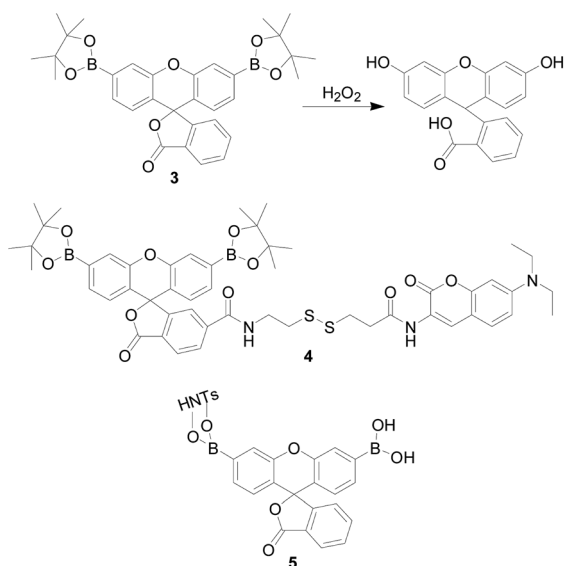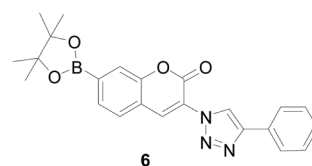

Fig. 6 Structure of fluorescent probe **6**.

hydrogen peroxide, and both have good selectivity. However, the sensitivity were not high, and the absolute fluorescence intensity was low, which affected the test in cells imaging. In recent years, more and more fluorophore was used as the framework of the probe.

In 2014, Shijun Shao's group[45] reported a case of BODIPY derivatives 7 (Fig. 7), which were synthesized by introducing 4-(bromomethyl)benzeneboronic acid pinacol eater moiety, and showed good solubility in water and "turn-on" fluorescent probe for the discrimination of H_2O_2. Probe 7 expresses excellent response toward H_2O_2 among the various ROS or RNS and biologically relevant species. Before binding with H_2O_2 the probe hardly had fluorescence due to the photo-induced electron transfer (PET) progress. Incubation of probe with H_2O_2 would release fluorophore, and the fluorescence of BODIPY was restored. Furthermore, the probe was successfully applied for both *in vitro* and *in vivo* imaging of H_2O_2 using cells and angelfish. In 2016, this research group[46] designed and synthesized another H_2O_2 fluorescence probe 8 (Fig. 7), which also based on borate ester hydrolysis mechanism. Similar to the luminescence mechanism of probe 7, before binding with H_2O_2 probe 8 showed no fluorescence due to the PET effect, and the PET effect disappeared after the reaction with H_2O_2, the fluorescence of carbazole group was recovered. Moreover, probe 8 has excellent selectivity and only H_2O_2 shows significant fluorescence enhancement. Other ROS or RNS, such as HOCl, O_2^-, ·OH, NO, ONOO$^-$, and GSH, ascorbic acid, glucose do not initiate or cause only minor changes. The probe has been successfully applied for monitoring and imaging of endogenous H_2O_2 in HeLa cells under physiological conditions. In addition, the structural modification of the carbazole pyridinium core provides a unique fluorescent material that opens the way for the construction of new fluorescent materials with unique optical properties.

Based on the PET mechanism, Weiying Lin's group[47] synthesized a fluorescent "turn-off" probe 9 (Fig. 8), which introduced carbazole-based fluorophore as a fluorescent dye and have PET process after reaction with H_2O_2. But unlike the above PET probe, there was no PET effect in the molecule before
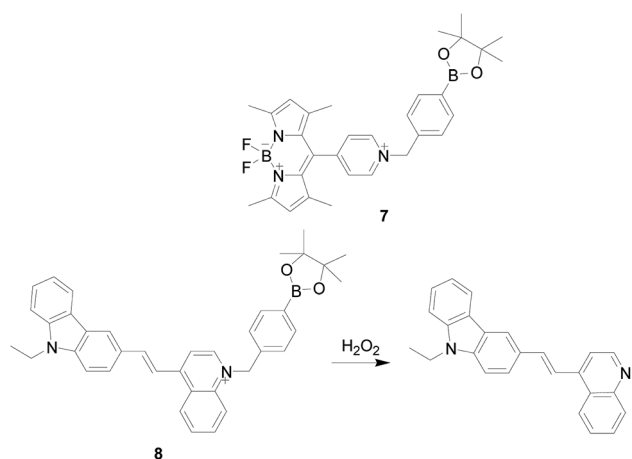

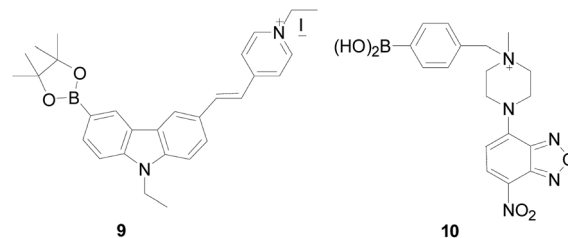
Fig. 8 Structures of probes 9 and 10.

combined with H_2O_2. Probe 9 displayed strong green fluorescence before reaction with H_2O_2 but showed low fluorescence after reaction with H_2O_2. The probe has a large Stokes shift (157 nm in water) in various solutions, which can maintain the accuracy of bioimaging, minimize the self-quenching effect, and achieve highly sensitive detection of H_2O_2 in aqueous solution. The next year, Xiaowei Xu's group[48] designed probes 10 (Fig. 8), in that they introduced 4-chloro-7-nitro-1,2,3-benzoxadiazole as the fluorophore core, and aryl boronate as a specific H_2O_2-reactive group. Upon exposure to H_2O_2 probe 10 exhibited distinct "turn-off" behaviors, and could be used in both neutral and alkaline aqueous conditions.

Although many probes for detection of H_2O_2 have been explored, rapid response probes are still expected. Based on intramolecular charge transfer (ICT), Wang and co-workers[49] synthesized fluorescent probe 11 (Fig. 9), which applied phenanthroimidazol, benzonitrile, and phenyl boronate as the three-component. Through introduction of benzonitrile as an electron-withdrawing group formation of a push–pull molecular mechanism modulation ICT process of probe 11, it can be detected H_2O_2 with good sensitivity not only *in vitro* but also *in vivo*. Moreover, compared to H_2O_2, probe 11 has high selectivity and negligible interference with other substances, including peroxyacetic acid (CH$_3$COOOH), ·OH, O_2^- and HOCl. The probe 11 can image H_2O_2 in the peritoneal cavity of mice. However, the emission is at blue, so it was not perfect to used *in vivo*.

There is increasing evidence indicating that lysosomes are important site for H_2O_2 production under both physiological and pathological conditions. Therefore, to design and synthesis of targeted H_2O_2 probe molecules is more important for the application of probes in organisms. In 2016 and 2017, Yibing Zhao's group[50,51] designed two lysosomal-targeted H_2O_2 probes 12 and 13 (Fig. 10). Probe 12 is a pH-switchable fluorescent H_2O_2-probe that responds sequentially to intracellular H_2O_2

Fig. 7 Structure of probe 7 and the mechanism of probe 8 with H_2O_2.
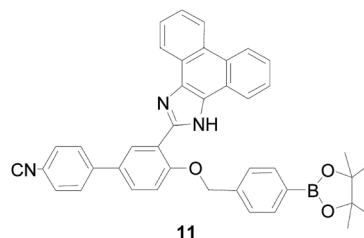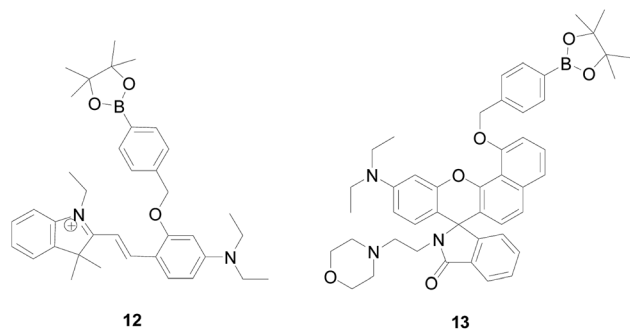

Fig. 9 Structure of probe 11.

Fig. 10 Structures of probes **12** and **13**.

and lysosomal pH, enabling the detection of the overall level of intracellular H_2O_2 by detecting the fluorescent signal intensity of lysosomes. This was because that probe **12** possesses a spirobenzopyran fluorophore emitting strongly at lower pH, showing high specificity to H_2O_2 and used for live cell imaging. The sensing strategy enables the visualization of the intracellular H_2O_2 through the lysosome windows more specifically, providing a new strategy for the spatially confined imaging in certain cell regions. Whereas, probe **13** is a novel acid activating probe with the same benzorhodol fluorophore as the probe described above. Probe **13** exhibits higher fluorescence intensity and longer emission wavelengths to H_2O_2, showing that **13** is more suitable for the monitoring of H_2O_2 under acidic conditions compared to Lyso-B-L2 and Lyso-B-L3. The fluorescence response of probe **13** to H_2O_2 and H^+ is highly selective, while the presence of other ROS, small bio-thiols, and metal ions does not cause a change in fluorescence. It is worth noticing that probe **13** uses morpholine as a localization group to provide pK_a suitable for lysosomal environment and efficient lysosomal localization ability. The probe is capable of fluorescently sensing endogenous lysosomal H_2O_2 in living cells, without signal interference from cytoplasm and other intracellular organelles.

The probe **14** (Fig. 11) was designed by Bo Tang's group,[52] which is a powerful tool for monitoring H_2O_2. The probe based on the aggregation induced luminescence (AIE) mechanism. When H_2O_2 was present in the system, the benzoborate groups in the probe were transformed into phenol groups, which increased the tetraphenylethylene aggregation. Upon reaction with H_2O_2, the fluorescence intensity of the probe **14** increased at 500 nm and reached a maximum value within 10 minutes. Probe **14** displayed a high selectivity toward H_2O_2 and a linear relationship with the concentration of (10–200 μM), and the detection limit was as low as 0.52 μM. Based on the above advantages, probe **14** has successfully applied to the imaging of RAW264.7 cells in mice. One of the most significant advantages of AIE-active probes is that they can applied to different conditions. For example, they can workable in solutions, aggregated and even solid states. Based on this, Benzhong Tang's research group[53] synthesized probe **15** (Fig. 11), which introduces phenylboronic pinacol ester on the AIE fluorogens (AIEgens). The same as probe **14**, when combined with H_2O_2 the probe's benzoborate groups were transformed into phenol. At
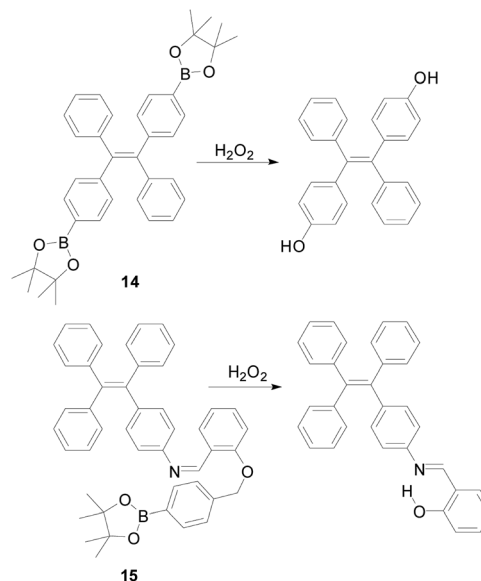
Fig. 11 Reaction of probes **14** and **15** with H_2O_2.

the same time, the probe forms a product with bright yellow fluorescence and the hydrogen bond in the product interact to detect of hydrogen peroxide with high sensitivity and high selectivity. The probe can also detect the concentration of glucose. The detection limit of probe **15** is as low as 100 nm, which is more sensitive than probe **14**.

Yang and colleagues[54] loaded a triarylboron-based AIE fluorophore on poly-urethane nanogel achieved probe **16** (Fig. 12). The boronate group can functionalize the triarylboron compound and give it the property of a fluorescence probe, which can provide continuous responses to H_2O_2. In addition, the introduced boronate group can also endow the triarylboron compound with AIE properties based on the dark TICT mechanism. By incorporating **16** into a polyurethane nanogel, they successfully utilized its photophysical properties to achieve a ratio readout for H_2O_2, and cells imaging can experience a color change from yellow green to blue green, which makes it suitable for potential applications in biology and medicine.

Hydrolysis of benzoborate ester groups was also used, Weiying Lin's research group[55] designed probe **17** (Fig. 12). In this probe, the double bond and benzene were used as a connector to connect the electron donor (*N*,*N*-dimethylamino) and electron acceptor (pyridinium cations), which can make the
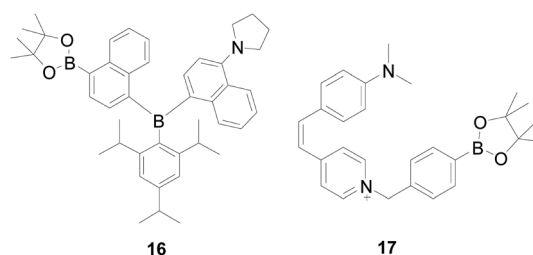

Fig. 12 Structures of probes **16** and **17**.

molecular free rotation in the excited state. Because the ability of pyridinium cations has a significant change in the probe **17** before and after reacting with H_2O_2, the excited state of the reaction product could not form the twisted internal charge transfer (TICT) state, the product have a strong fluorescence emission. The probe's emission intensity and the concentration of H_2O_2 in range of 0–30 μM shows a linear relationship. The probe **17** showed a highly sensitivity and the detection limit was 2.1×10^{-6} M which is sensitive enough to determine the H_2O_2 level of the lesion. Moreover, probe **17** is more selective for H_2O_2 than other reference species such as ROS/RNS. In addition, pyridinium cation, as one of the mitochondrial targeting groups, possesses superior membrane permeability and can rapidly enter the mitochondria in cells in a short time. The discovery of this probe laid the foundation for future research on Alzheimer's disease. Based on similar mechanism, Xueping Feng's group[56] synthesized a probe HPQB, which also can detect H_2O_2 and glucose in cells.

In 2018, Zhou Bo's group[57] reported a probe **18** (Fig. 13), which introduced another mitochondrial targeting group alkylated triphenylphosphine in it. Probe **18** is specific for H_2O_2, with only H_2O_2 inducing significant fluorescence enhancement, while other ROS and RNS triggering no or limited changes. In addition, probe **18** demonstrated excellent water solubility and applied under physiological pH condition along with low cytotoxicity, and tracked of mitochondrial H_2O_2 in living cells. Therefore, the probe was expected to use as a tool to explore the biological effects of mitochondrial H_2O_2, and to facilitate the study of mitochondrial-targeted anticancer drugs. As early as 2008, the probe **19** (Fig. 13) was designed and synthesized by Chang's research group,[39] which introduced triphenylphosphine as a mitochondrial targeting group. Probe **19** could selectivity detect H_2O_2 in the mitochondria of living cells over other ROS like ·OH, O_2^-, NO. Moreover, the level of H_2O_2 in mitochondria of various mammals and the increase of H_2O_2 caused by oxidative stress in Parkinson's disease model can be observed through imaging changes.

In order to reduce background interference and cell damage, enhance optical transparency of tissue and the ability to interrogate thicker specimens, it is increasingly important to design and synthesize probes that can emit spectra in the visible far-red to near infrared-region. Chang's group[40] synthesized probe **20** (Fig. 14), which is a new borate-based red-emitting fluorescent indicator for H_2O_2. The probe was capable of responding to changes in exogenous H_2O_2 levels within RAW264.7 cells. However, as the absolute fluorescent brightness of
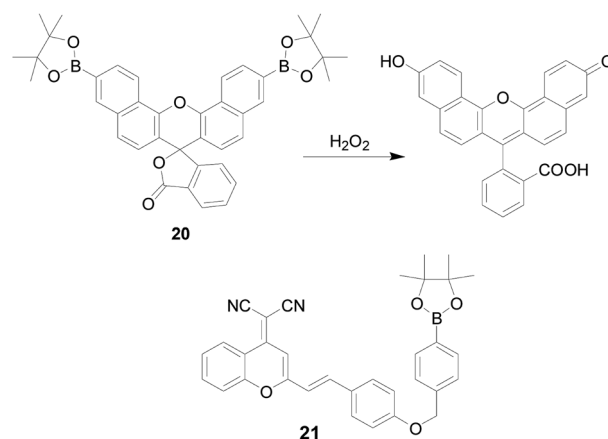

Fig. 14 Reaction of probe **20** with H_2O_2 and the structure of **21**.

naphthofluorescein was weaker than fluorescein and other fluorophore used previously, attempts to use this probe to study oxidative stress in cells have failed. Haitao Li's team[58] designed a new near-infrared probe **21** (Fig. 14) with dicyanomethylene-4H-pyran moiety as fluorophore and borate ester as the recognition unit. The probe was "turn-off" response based on the ICT mechanism. After probe **21** was cultivated with H_2O_2, the recovery of the ICT process resulted in an obvious increase in fluorescence emission at 688 nm, accompanied by a distinct color change from yellow to purple, revealing the feasibility of "naked-eye" monitoring H_2O_2. Encouraged by the properties of near-infrared emission, probe **21** was successfully applied in the imaging of exogenous and endogenous H_2O_2 in HepG2 cells.

Liyi Zhou's group[59] constructed a two-photon near-infrared fluorescent probe **22** (Fig. 15), which introduced the oxonium ion as the mitochondrial targeting unit and phenylboric acid as the H_2O_2 reaction moiety. Probe **22** could successfully applied for H_2O_2 imaging of liver tissue up to 170 μm depth in red fluorescence channels. After reacting with H_2O_2, the fluorescence intensity of probe **22** increased significantly by more than 105 times at the emission wavelength of 665 nm, which is much larger than other ROS, which meets the selectivity requirements of practical applications. Furthermore, the probe has good dyeing ability and high penetrating ability to H_2O_2 image tissue, and can be applied to liver tissue H_2O_2 images with a depth of 50–170 μm in a red fluorescent channel.

More and more borate fluorescent probes were used to detect hydrogen peroxide in cells. However, most of these probes were single-photon imaging technology. In addition to the
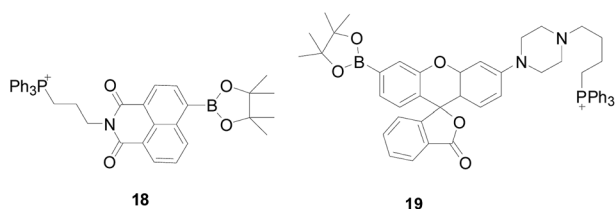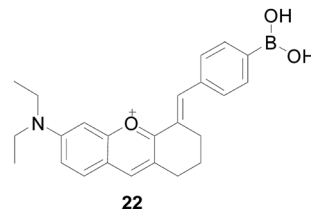

Fig. 13 Structures of probes **18** and **19**.

Fig. 15 Structure of probe **22**.

description above, there were many probes designed using this technique.[60–70] The photo-damage and photo-bleaching properties of single photon imaging technology have prevented long-term imaging during bioimaging process, and it has strong background interference and low UV transmittance, which limits their applications in deep tissue imaging. By contrast, two-photon (TP) fluorescent probes can greatly overcome these defects. By using near-infrared (NIR) lights as the excitation source, the two-photon fluorescent probes can reduce the photo-damage and photo-bleaching caused by single-photon fluorescent probes, increase tissue penetration, and promote three-dimensional imaging of living tissue. Hence, the two-photon probes are more suitable for biological detection and imaging, providing sharper tool for life science research.

Probe **23** (ref. 71) (Fig. 16) was the first developed and reported two-photon fluorescent probe for H_2O_2, which introduced a boronate-based carbamate leaving group to 2-acetyl-6-aminonaphthalene (AN1), designed by Bong Rae Cho and co-workers, suitable for deep tissue imaging. After adding H_2O_2 to the solution, probe **23** was converted into AN1. Probe **23** can be excited by 750 nm femto-second pulses, showing a significant TP cross section, a marked blue-to-green emission color change in response to H_2O_2, good ROS selectivity, and insensitivity to pH in the biologically. In addition, probe **23** was capable of visualizing H_2O_2 levels in both RAW264.7 cells and tissue models at depths of 90–180 mm without interference from other biologically relevant species. In order to study the complex relationship between lysosomes and physiological H_2O_2, Weiying Lin's team[72] developed a fast-response and lysosomal targeted two-photon fluorescent probe **24** (Fig. 16), which has a relatively high targeting effect on lysosomes. The probe itself has an "A–π–A" structure, and after reacting with H_2O_2, the borate group becomes a hydroxyl group (electron donating group), and its electronic structure becomes donor–π–acceptor "D–π–A" structure. This change shows a distinct fluorescence on signal with an 80-fold increase in fluorescence signal, which is attractive for H_2O_2 imaging in living tissue with deep tissue penetration. Qiujuan Ma's team[73] synthesized a highly selected two-photon fluorescent probe **25** (Fig. 16) for H_2O_2, based on a naphthalene platform and a boric acid ester H_2O_2 response site. Naphthalene backbone with a D–π–A structure, which can improve fluorescence quantum yield and photochemical stability. Probe **25** has good selectivity to H_2O_2, and only H_2O_2 can cause strong fluorescence intensity

enhancement at 505 nm, while other ROS substances will not, including $ONOO^-$, O_2^-, ClO^-, $\cdot OH$, tert-butylhydroperoxide (TBHP), $^1O_2$ and NO. It could be applied for quantitative detection of H_2O_2 in live cells and tissues with good cell-permeability, and the detection limit was 0.7 μM. The ointment is that the probe's response time is long and the sensitivity was not wonderful, which requires a further improvement.

Two-photon fluorescence probes for bio-detection and imaging reported in the literature,[74] the two-photon absorption cross section of most probes was not very satisfactory, and needs further development to improve the sensitivity of detection and the clarity of imaging, and broaden the biological range of imaging. Fluorescence ratiometric eliminates the effects of source intensity and instrument sensitivity. After the probe was combined with H_2O_2, the fluorescence intensity ratios measured at two different wavelengths can be calibrated to overcome the artifacts of the fluorescent signal due to changes in ion concentration.

Subsequently, Bong Rae Cho research group[75] designed and reported probe **26** (Fig. 17), the first two-photon probe for ratiometric detection of H_2O_2, which introduced triphenyl-phosphonium salt as the mitochondria-targeting site, could detected H_2O_2 level change in mitochondrial in cellular environments and intact tissues at depth >100 μM. After adding 1 mM H_2O_2 to a solution of 1 μM probe **26**, the ratio (F_{yellow}/F_{blue}) of fluorescence intensity increased by 75-folds. Hwan Myung Kim's team[76] used a carboxyl group to replace the triphenylphosphine in probe **26** and synthesized the probe **27** (Fig. 17), which also showed a change in fluorescence color from yellow to blue in response to H_2O_2. The ratio two-photon microscopy of **27** images displayed that H_2O_2 levels gradually increased from brain to kidney, skin, heart, lung, and then liver tissue. In addition, the above two probes exhibited higher selectivity for H_2O_2 than competitive biological species, ROS and RNS, and the ratio of F_{yellow}/F_{blue} is unperturbed after adding diverse ROS and RNS, including TBHP, O_2^-, HOCl, NO, $\cdot OH$, tert-butoxy radicals ($\cdot OtBu$) and $ONOO^-$. These results indicate that this type of probe will be useful for application in studies of biological and medical research.

Chunhua Fan and colleagues[77] reported a two-photon H_2O_2-specific fluorescent probe **28** (Fig. 18), which based on the ICT mechanism, with 6-hydroxy-2,3,4,4a-tetrahydro-1H-xanthen-1-one (TX) as a fluorophore. The probe **28** has a fast fluorescence response to H_2O_2 in 9 minutes, which with high sensitivity, high selectivity and biocompatibility. This probe has been successfully used for imaging H_2O_2 in mouse liver tissue. Manoj Kumar and colleagues[78] also published a charge transfer
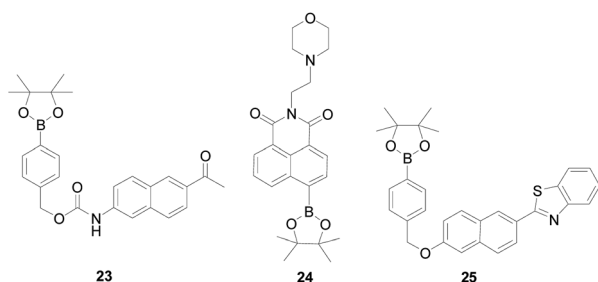

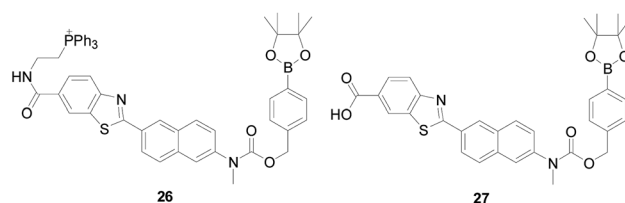Fig. 16   Structures of 23, 24 and 25.

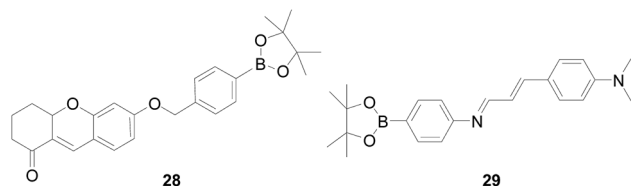Fig. 17   Structures of fluorescence probes 26 and 27.

Fig. 18 Structures of fluorescence probes **28** and **29**.

assisted fluorescent probe **29** (Fig. 18), the dimethylamino group is protonated, inhibiting the twisted intramolecular charge transfer from the dimethylamino group to the imine moiety, which causes the emission at 566 nm to disappear and the higher energy emission occurring at 484 nm. In the case of the **29**-H_2O_2 system, the fluorescence intensity ratio of I_{484}/I_{566} is 9.5-times. It can be said that the probe **29** is H_2O_2-specific, and no significant change is observed in other reactive oxygen species. In summary, this probe can detect H_2O_2 in prostate cancer (PC3) cell lines *in vitro*, exploring the potential biological applications of probe.

The fluorescence probe designed with the change of fluorescence intensity at a single wavelength is easily interfered by external factors such as equipment efficiency, environmental conditions and probe concentration, so as to reduce the selectivity and sensitivity of fluorescence probe detection. In contrast, the ratiometric fluorescent probes can overcome these shortcomings by allowing simultaneous detection of two signals resulting from reacted and unreacted forms of the probe in the same sample.

Chang' group[79] designed a ratiometric fluorescent probe **30** (Fig. 19), which exhibited a blue fluorescence emission at 475 nm, after the interaction with H_2O_2, its emission wavelength was red shifted to 540 nm by ICT mechanism, resulting in a 12-fold change in the ratio (F_{540}/F_{475}). Using the ratiometric property of **30**, the authors studied the changes of H_2O_2 in RAW264.7 cells under stimulated by PMA, found that after probe **30** induction, the fluorescence changes in phagocytic vesicles were more pronounced than in other parts of the cell, which indicated that H_2O_2 was produced during phagocytosis.
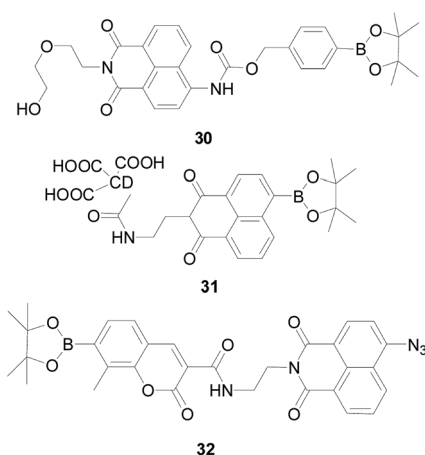
Shuizhu Wu's research group[80] developed a nano-fluorescent probe **31** (Fig. 19) based on FRET mechanism, which was stable in spectral properties and easy to modify. Probe **31** is capable of selectively detecting the fluorescence intensity ratio (I_{550}/I_{457}) in the presence of H_2O_2 and other potentially competitive ROS/ RNS. With the concentration of H_2O_2 increases, the fluorescence ratio (I_{550}/I_{457}) increased steadily. In addition, the coexistence of other species does not affect the detection of H_2O_2. As an energy donor and carrier for H_2O_2 recognition, carbon dots (CD) have good biocompatibility.[81] CD-based nanoprobes are small in size and low in toxicity, and can respond quickly to H_2O_2, which is beneficial *in vivo* detection. The probe **31** is currently capable of monitoring and localizing endogenous H_2O_2 in zebrafish caused by oxidative damage to the drug.

Also based on FRET mechanism, Shubao Wu's group[82] developed a fluorescent probe **32** (Fig. 19), which combined two different fluorophores (coumarin and naphthalimide) forming a two-channel imaging method through dual sensing strategies to detect H_2S and H_2O_2 in living cells, which can be applied to diagnose cancer. This dual response strategy overcomes the uneven distribution of dual probes, providing accurate information about multiple analytes within the cell, and encourages the development of more fluorescent markers for detecting multiple analytes to label cancer cells.

In recent years, the development of near-infrared and multiphoton quantitative detection of ratiometric probes has become a new trend, with its unique background interference, no biological tissue damage and other unique properties, attracting a wide range of academic attention.

Xiangzhi Song and Wenqiang Chen[83] combined the ICT and ESIPT mechanisms to design a novel mitochondria-targeted fluorescent probe **33** (Fig. 20) that showed a red fluorescence ratio of $I_{594\ nm}/I_{666\ nm}$ at a single excitation wavelength of 440 nm. Unlike other benzothiazole-based ratio probes, probe **33** reacts with H_2O_2 to suppress the ICT process, exhibiting a large stoke shift (from 102 nm to 254 nm) and a significant ratio of fluorescence changes. Large Stokes shifts can minimize self-absorption and auto-fluorescence interference. Moreover, it can improve detection sensitivity, and facilitate biological cell
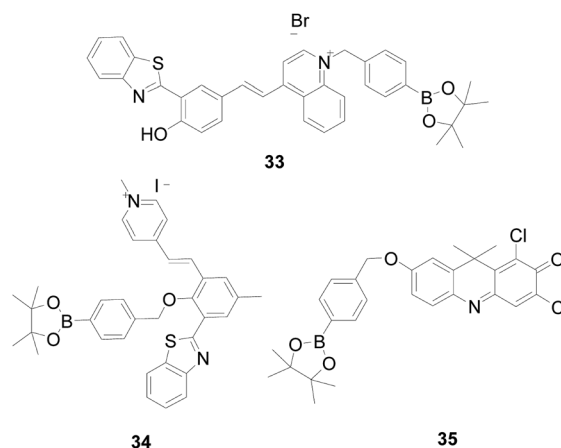

Fig. 19 Structures of probes **30**, **31** and **32**.

Fig. 20 Structures of probes **33**, **34** and **35**.

imaging. Lijun Tang's team[84] also developed a near-infrared mitochondria-targeted ratiometric probe **34** (Fig. 20) with a large stoke shift (357 nm), good sensitivity and selectivity, and has been successfully applied for A549 cell imaging.

By adjusting the intramolecular charge transfer process of dye 9H-1,3-dichloro-7-hydroxy-9,9-dimethylacridine-2-one (DDAO), Yuguang Song's team[85] synthesized a ratio-type "turn-on" near-infrared probe **35** (Fig. 20) with high sensitivity and low background interference. Probe **35** produces a strong orange fluorescence emission at 620 nm, which was converted to DDAO after H_2O_2 response, and the wavelength is red shifted to 660 nm with red fluorescence. Except for H_2O_2, no palpable improvement in the fluorescence ratio (F_{660}/F_{620}) were observed for biological relevant ROS/RNS, GSH, Cys, VC, cations and amino acids. The probe satisfies the need for quantitative monitoring of H_2O_2 in the body.

Phenylborate is a classical group that recognizes H_2O_2 and has made outstanding contributions to the study of H_2O_2. However, the reaction of phenylborate to H_2O_2 also has certain disadvantages. Firstly, although a large number of ratiometric probes[86–88] have been designed for the quantitative detection of H_2O_2, the concentration change of H_2O_2 cannot be monitored in real time. In addition, in recent years, there have been reports in the literature[89–91] that phenylborate can react with $ONOO^-$ and ClO^-, and the reaction rate is much faster than that with H_2O_2.

Therefore, developing and synthesizing high-selectivity, high-sensitivity, fast responding fluorescent probes for H_2O_2 based on new response groups is a significant and challenging task.

3. Sulfonate-based fluorescent H_2O_2 probes

Similar to the response of the borate to H_2O_2, the sulfonate can also be used as a responsive group for H_2O_2.

In 2004, Maeda and co-workers[92] first discovered pentafluorobenzenesulfonyl fluorescein derivatives **36a–c** (Fig. 21) as novel selective fluorescent probes for H_2O_2 with a sulfonate as a responsive site. The fluorescent precursor of the probe has a high fluorescence quantum yield; the sulfonate is more stable than the general ester and not easily hydrolyzed; the structure of the pentafluorobenzene ring increases the reactivity of the probe with H_2O_2. After H_2O_2 reacts with the probe **36**, the sulfonate was hydrolyzed to release fluorescein, and the

fluorescence is enhanced. The fluorescence response intensity of this series of probes was also positively correlated with the temperature. As the temperature increased, the detection limit decreased.

Tang Bo's group[93] presented a disulfonate-responsive probe **37** (Fig. 22) as a fluorescent imaging agent to monitor intracellular H_2O_2. Probe **37** is an excellent naphthalene-based fluorescent reagent. Compared with fluorescein, the stent has red-shifted spectral characteristics. After treatment with various concentrations of H_2O_2, the probe produces a linear fluorescence response with a low detection limit, good selectivity, reported as a smart probe for H_2O_2 in mouse peritoneal macrophages. The same group designed probe **38a** and **38b** (ref. 94) (Fig. 22), which was based on the mechanism of H_2O_2-mediated hydrolysis of sulfonates. The probes introduced two sulfonate groups into the fluorescein chromophore as response sites. Fluorescence experiments showed that probes **38a** and **38b** had excellent selectivity to H_2O_2 over other intracellular ROS and some biological compounds and low detection limit. In addition, the probes based on sulfonate were cell permeable, which can detect the micromole change of H_2O_2 concentration and observe living cells with confocal microscope. In consideration of the excellent performance of the probe, the study was conducted to detect both H_2O_2 and superoxide in pleural lavage fluid and lung cells. The study was conducted on Wistar rats with bleomycin-induced pulmonary fibrosis. The signal transduction system for determining the content of H_2O_2 was developing.

Since the induction of H_2O_2 by the fluorescent probe acts based on the different reaction process, the sensitivity of the probe is greatly affected by the reaction rate. It is difficult to improve the reaction rate by changing the chemical structure of the single-molecule probe system. However, as has been reported,[93] it can be known that real-time imaging of intracellular H_2O_2 can be achieved by using a switchable photoluminescent inorganic nanoprobe. Considering the reaction kinetics, Soo Young Park and Sehoon Kim[95] devised a simple method to catalyze the sensing reaction by binding a fluorescent probe to a nanoreactor through a catalyst, so that the imaging of H_2O_2
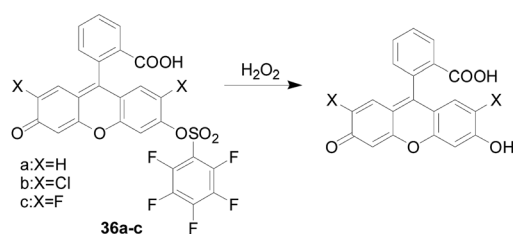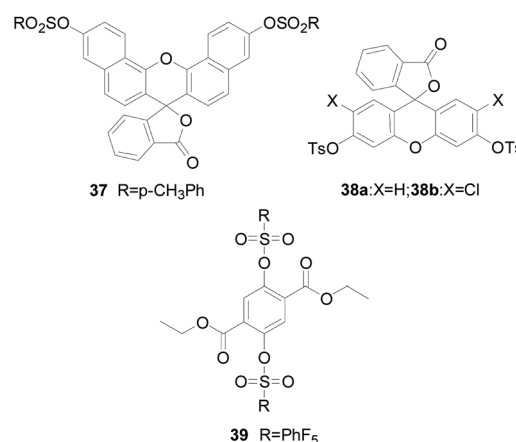

Fig. 22 Structures of probes **37**, **38** and **39**.

Fig. 21 Reaction of probe **36a–c** by H_2O_2.

has improved spatiotemporal resolution during cellular process. The method was proposed entirely based on the hydrolysis of the new probe **39** sulfonate group (Fig. 22), which showed a "turn-off" fluorescence response and real-time imaging of H_2O_2.

Recently, Fabiao Yu's team[96] developed a near-infrared ratio fluorescent probe **40** (Fig. 23). The probe **40** itself showed the maximum absorbance centered at 830 nm, with the increase of H_2O_2, the fluorescence intensity decreased gradually, and a new absorption peak appeared at 635 nm, which had an excellent linear relationship. The ratiometric signals showed negligible changes for these reactive species including various ROS/RNS (HOCl, ·OH, $^1O_2$, O_2^-, NO and $ONOO^-$) and mercaptan (GSH, Cys, and Glu). The team used the probe **40** to examine the critical role of endogenous H_2O_2 in cell proliferation in viable hippocampal neurons and successfully demonstrated a close association between changes in endogenous H_2O_2 levels and brain development at different stages.

4. Benzoyl-based fluorescent probes for H_2O_2

In 1979, S. Foote team[97] elaborated the reaction mechanism of benzil with H_2O_2, as shown in the Fig. 24. At the beginning, H_2O_2 nucleophilic attack on the carbonyl of benzil, then the Baeyer–Villiger reaction occurs to form an unstable intermediate, and the intermediate is rapidly hydrolyzed to produce benzoic acid.

Nagano's group[98] described a fluorescent "turn-on" H_2O_2-probe **41** (Fig. 25) for the first time using benzil as a specific recognition group for H_2O_2. They synthesized 5-benzoylcarbonylfluorescein derivatives as candidate fluorescence probes using PET mechanism, finding that when the electron-withdrawing groups (–Br, –CN, and –NO_2) were attached to the benzil, the reactivity with H_2O_2 was significantly enhanced. The stronger the electron absorption of the group, the higher the reactivity of the probe **41**. The results demonstrated that probe **41** had the highest reactivity, better signal-to-noise ratio with H_2O_2, and the highest fluorescence enhancement ratio. Indeed, the enhancement of fluorescence intensity after reaction with hydrogen peroxide was as high as 150-fold. Compared with previously reported fluorescence probes utilizing benzenesulfonyl ester or boronate ester chemistry, the selectivity of probe **41** among ROS is unique. Which made probe **41** could be as a useful tool for biological detection. Experiments indicated that the probe could detect endogenous H_2O_2 produced by RAW264.7 macrophages and A431 human epidermal cancer
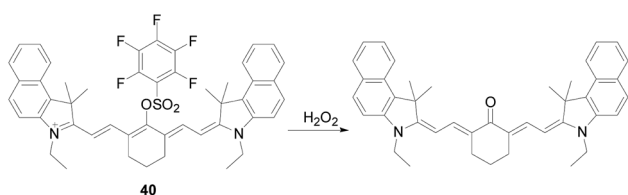

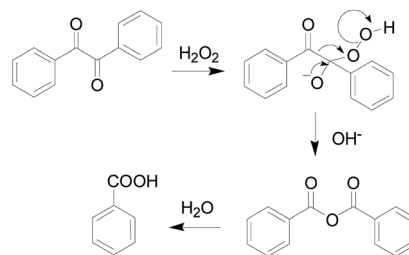Fig. 24 Reaction mechanism of benzil with H_2O_2.

cells. The design strategy used here applied not only to fluorescein derivatives, but also to other fluorophore. In 2014, Hideki Sumimoto research group[99] also designed and synthesized a fluorescent probe **42** (Fig. 25) with fluorescein as the nucleus based on the response mechanism of phenyldiethyl ketone, introducing a phage targeted positioning group benzyl guanine. It resulted in the formation of a fluorophore–protein conjugate that reacts rapidly with H_2O_2. Probe **42** rapidly reacted with H_2O_2 and showed a 9-fold increase in fluorescence intensity. Which successfully applied to monitor endogenous H_2O_2 produced during phagocytosis of RAW264.7 macrophages in real time.

Chen Jianbo and colleagues[100] designed new probes **43a** and **43b** (Fig. 26) using BODIPY as the fluorophore and benzil as the H_2O_2 recognition group. Investigating the fluorescent properties of **43a** and **43b**, finding that **43a** and **43b** successfully turn on highly green-emitting fluorescence, which satisfies "off–on" fluorescent probes to decrease background interferences. In addition, when they are reacting with excess H_2O_2 for 60 minutes, respectively, the fluorescence intensity of **43a** increased by 78 times, much higher than that of **43b** (70 times). The authors believe that the above results are because **43a** owns a more pronounced steric effect and weaker capacity of the electron withdrawing. Inspired by much better response of **43a** to H_2O_2, a further step was took to investigate other analytical capabilities of **43a**. Since the carboxyl product of **43a** reacts with
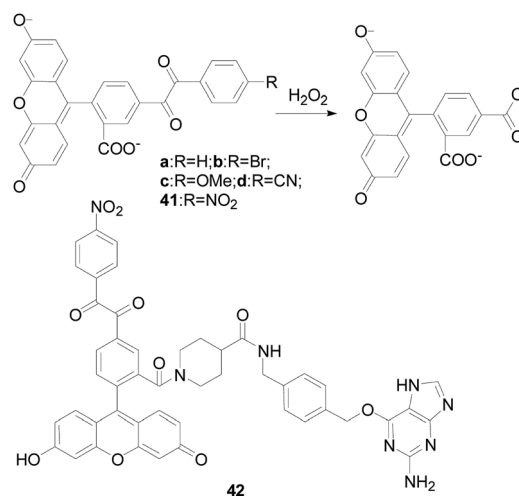

Fig. 23 Reaction of probe **40** with H_2O_2.

a:R=H;b:R=Br;
c:R=OMe;d:R=CN;
41:R=NO_2

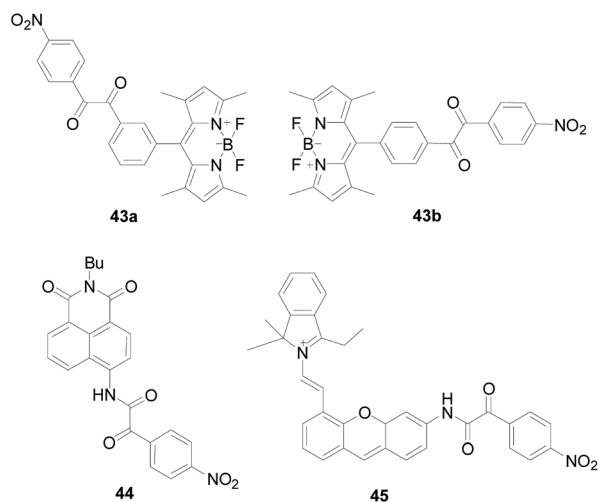Fig. 25 Reaction of probe **41** with H_2O_2 and the structure of **42**.

Fig. 26 Molecular structures of probes 43a–b, 44 and 45.

H_2O_2 to increase the adsorption capacity and sensing efficiency, probe 43a exhibits a fast response (30 s) and high sensitivity (0.94 ppb) to H_2O_2 vapor, and has a high fluorescence quantum yield of 0.43–0.56. Probe 43a is the first fluorescent probe could be successfully used for H_2O_2 vapor detection and has been used for the visual detection of H_2O_2 of vapor by naked-eye and fluorescence imaging in living cells. Almost at the same time, Sabrina Heng's team reported a probe[101] with the same structure as 43b and performed spectral analysis, selectivity and cell imaging experiments. The probe is highly selective for H_2O_2, and oocytes stained with probe showed a minor increase in fluorescence when treated with H_2O_2.

Zhang Xiaoling's group[102] published a ratio type fluorescent probe 44 (Fig. 26) for the targeted detection of H_2O_2 in the endoplasmic reticulum. The α-ketoamide in the probe was converted to an amine after reaction with H_2O_2, the new fluorescence emission peak gradually increased at 540 nm, and the peak at 465 nm gradually decreased. The probe 44 can quantitatively detected the content of H_2O_2 by the ratio method with highly selectivity, and eliminated the error caused by the probe concentration and environment. And realizes the detection of exogenous H_2O_2 in HeLa cells.

Using the same mechanism, Bo Tang's research group[103] developed a near-infrared fluorescent probe 45 (Fig. 26), which integration a unique reaction site α-ketoamide into a hemicyanine fluorophore. Probe 45 is a fluorescence "off–on" probe regulated by an ICT mechanism. Upon reaction with H_2O_2, hemicyanine-NH_2 was released and showed significant fluorescence enhancement attributing to the ICT process. Probe 45 has a high reaction rate and high specificity, and the fluorescence intensity at 704 nm in the fluorescence spectrum increases as the concentration of H_2O_2 increases, whereas other ROS or RNS no. The use of probe 45 confirmed the formation of H_2O_2 during ischemia-reperfusion injury at both cell organ levels.

In general, the above-mentioned benzil-responsive fluorescent H_2O_2 probe reacts more rapidly, and both used a nitro group as an electron-withdrawing group to enhance the reactivity of the probe. However, this type of ratio-type near-infrared

probe is not mature enough, and there is room for further research.

5. *o*-Benzenediol based fluorescent H_2O_2 probes

The *o*-diphenolic hydroxyl group is also a good response group for H_2O_2.

Hankley's team[104] introduced the synthesis and biological applications of a novel H_2O_2 probe 46 (Fig. 27). The *o*-diphenolic hydroxyl in the probe structure reacted with H_2O_2 to oxidize to *o*-quinone, which was a fluorescence quenching reaction, and the fluorescence intensity at 630 nm gradually decreased with the colour change from blue to purple of solution. Only a small fluorescence response was observed in the emission spectrum except for physiologically relevant levels of H_2O_2. As the GSH in the solution added, the fluorescence was turn on. Therefore, this "on–off–on" type of probe can monitor intracellular H_2O_2 oxidative stress and thiol-reduction repair processes simply and directly, and has good permeability and specificity in cells, negligible background fluorescence and cells toxicity.

As a further study in this field, in 2017, Manoj Kumar and colleagues[105] reported a lysosomal targeting H_2O_2 fluorescent probe 47 (Fig. 28), which comprised a catechol responsive group and a naphthalimide fluorophore. In that catechol can undergo PET effects to the naphthalimide core resulting in weak molecular fluorescence in aqueous solution. Upon addition of H_2O_2 to the aqueous solution of probe 47, the PET effects were inhibited and the emission band at 537 nm was enhanced. There was no obviously fluorescent response to other ROS/RNS like NO, TBHP, ·OH, and $OONO^-$ and bio-thiols like Cys, GSH and Hcy. The morpholino group in the probe 47 acted as a lysosomes-targeting group can be used for endogenous detection of H_2O_2 in living cell lysosomes, and can also be used to detect H_2O_2 in brain tissues and living nematodes.

6. Enamine-based fluorescent probes for H_2O_2

In 2018, Wang Peng's group[106] used H_2O_2 to promote the carbon–carbon double bond cleavage, and prepared a probe 48 (Fig. 29) with an enamine group as a reactive group. After the reaction of the compound 48 with H_2O_2, a peroxide intermediate formed, which is then converted to a stable amide with

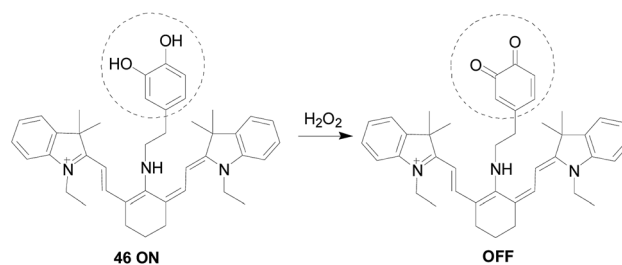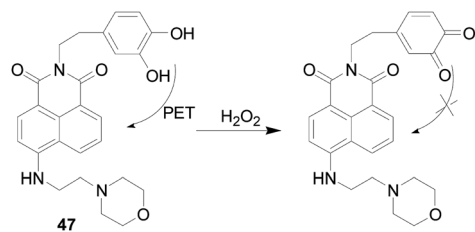Fig. 27 Reaction mechanism of probe 46 with H_2O_2.

**Fig. 28** Fluorescence response of probe **47** to H_2O_2.

Fig. 30 Reaction scheme of **49** and **50** with H_2O_2.

blue fluorescence emission with good sensitivity. The response of probe **48** to H_2O_2 was nearly 10–30 times than that of control group and other interference factors, such as various amino acids (Met, Glu, Cys, GSH) and ROS (TBPH, ClO^-, $\cdot OH$, NO, $ONOO^-$). Properly designed probes have great potential to monitor H_2O_2 in cells, mouse liver sections and tumor tissues using single-photon and two-photon fluorescence imaging with low cytotoxicity.
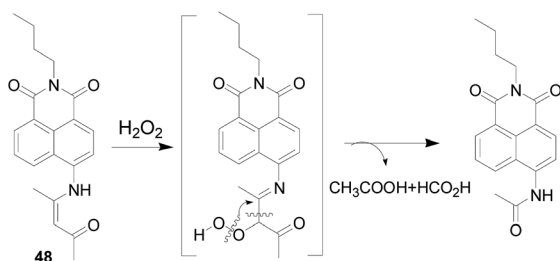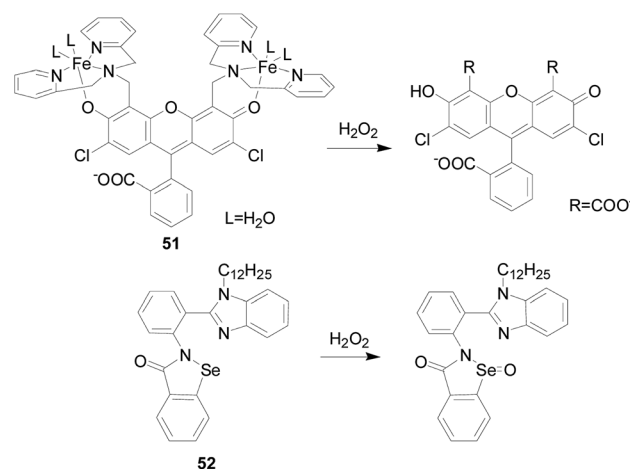
7. Other types probes for H_2O_2

Yutaka Hitomi's team[107] developed a metal-based probe **49** (Fig. 30), which produced a fluorescent response faster than an organic molecular-based fluorescent probe, showing significant fluorescence enhancement in 20 seconds. The Fe complex in this probe reacted rapidly with H_2O_2 to form a cationic amide group by three routes. Hydrolysis of the cationic amide group by an iron(III)-bound hydroxo group or an unbound water molecule finally gives resorufin and a hydrolyzed iron complex, $[Fe^{III}(3)]^{2+}$. Resorufin produces significant red fluorescence. The authors applied it to the detection of H_2O_2 produced during the enzymatic reaction. Since probe **49** may be hydrolyzed by amidate under cell culture conditions, which hinders its application to fluorescence imaging of intracellular H_2O_2. In order to fully enhance the stability of the metal complex H_2O_2 probe to visualize intracellular H_2O_2, the group developed a new iron complex-based probe **50** (ref. 108) (Fig. 30). The group employs the nonheme iron-based peroxidase mimetic Fe(III) mpaq (mpaq = 2-[N-methyl-N-pyridin-2-ylmethyl]-amino-N′quinolin-8-yl-acetamido) as a H_2O_2-responsive component, in which the iron complex reacts rapidly with H_2O_2 to form an oxidant substance that converts the closely appended o-alkyl resorufin moiety to resorufin. Probe **50** showed a strong enhancement in fluorescence intensity in response to H_2O_2, which was much
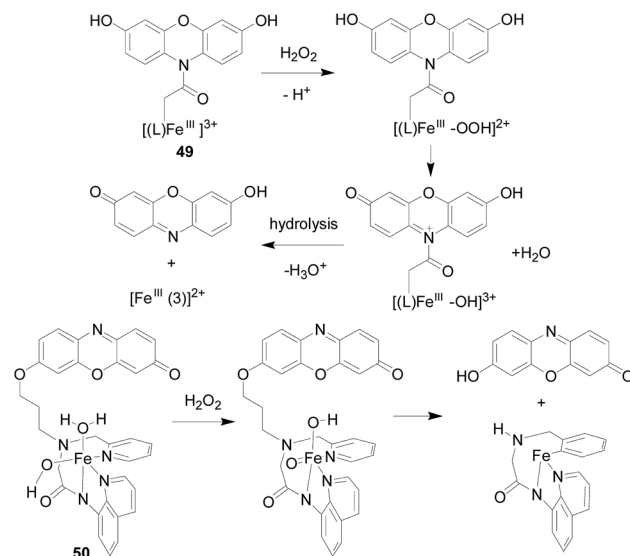
stronger than other oxidants such as $\cdot OtBu$, O_2^-, NO and ClO^-. Experiments have shown that probe **50** is suitable for H_2O_2 imaging produced by EGF stimulation.

Youngmin You's team[109] developed a new fluorescent probe **51** (Fig. 31) for H_2O_2 based on the cleavage of a paramagnetic Fe ionophore from a fluorophore. By dissociation of the Fe-ionophore, probes **51** reacts with H_2O_2 produces 2,7-dichlorofluorescein, rather than other oxidants derived from H_2O_2 (e.g., $\cdot OH$). Almost no response was observed for O_2^-, HOCl, t-BuOOH, NO, $^1O_2$, and only a limited increase in the fluorescence intensity was observed in the cases of t-BuOOH and $\cdot OH$. Moreover, the probe **51** is suitable for live cell imaging and has the ability to detect intracellular H_2O_2 in lysosomes.

Xiaoqi Yu's research group[110] designed and synthesized a "turn-on" type fluorescent probe **52** containing selenium. Under the action of H_2O_2, the selenium atom was oxidized to selenium oxide, and the effect of PET itself was inhibited,

Fig. 31 Reaction mechanism of probes **51** and **52** with H_2O_2 respectively.

Fig. 29 Mechanism of probe **48** to H_2O_2.

forming aggregates and AIE-type fluorescence occurred. The fluorescence intensity of probe **52** was proportional to the H_2O_2 concentration, more than 110-fold fluorescence enhancement was observed after treatment with 200 μM H_2O_2 for 1 h at ambient temperature. Other ROS/RNS, including ClO^-, TBPH, $ONOO^-$, ·OtBu, ·OH, $^1O_2$, and O_2^-, could not cause the fluorescence change of the probe **52**.

8. Concluding and outlook

The production, decomposition and diffusion of hydrogen peroxide are unstable in different cells. It is important to develop a highly sensitive hydrogen peroxide probe for real-time *in situ* detection of H_2O_2 in cells or organisms.[111] The development of fluorescent probes provides a versatile and valuable way of thinking about the processes behind many biological phenomena in living systems. Among the most H_2O_2 probes, the development of fluorescent probes is the most extensive because of their better biocompatibility and higher sensitivity.

This review summarizes several commonly used small molecule types of H_2O_2 fluorescent probes, such as based on aryl borate or boric acid, sulfonate, benzoyl and the like. These fluorescent probes are able to overcome the nature of hydrogen peroxide itself and have high sensitivity and specificity for H_2O_2. The probes developed in recent years combined with confocal microscopy and micro-spectral detection technology have been able to perform "real-time, visible, quantitative" detection of hydrogen peroxide in living cells and tissues. In spite of that, the development of probes requires further consideration of the following issues. Since the same recognition moiety that adapts to different fluorophores will exhibit specificity for different targets, an in-depth study can be performed based on the structure–reactivity relationship of the reported probes to derive intrinsic rules that guide the targeted design and synthesis of the probe. Although the detection of endogenous H_2O_2 *in vivo* can be obtained, the imaging depth is still limited due to the light penetrating ability and the stability of the probe. Due to the low background interference and weak photo-bleaching effects, ratiometric and TP-probes have great bio-imaging potential for H_2O_2 and can be used as sensing platforms, but this only helps solve some of the problems, not all. In general, these issues not only provide researchers with challenges, but also the opportunity to enter new research areas.

Therefore, in the development of the probe, considering the relatively low concentration in steady state of H_2O_2 in the body, it needs to be designed from both chemical and biological aspects. On the one hand, we need to find more reaction mechanisms (currently based on oxidation reactions). On the other hand, in addition to considering high selectivity and sensitivity, low auto-oxidation, high optical stability, low cytotoxicity, good solubility, cell permeability, and low interference of biological environmental substances need to be considered. In addition, since redox reactions are involved in the maintenance of normal function and health of cells, it is also a research focus of fluorescent probes to study redox probes of cellular redox biology by monitoring changes in reversible fluorescence over time.

In summary, the search for probes that better reflect the physiological and pathological functions of H_2O_2 in cells and organisms will be one of the important hotspots and difficult areas of current life science research. We believe that with the development and further integration of novel small molecule fluorescent probes in related fields such as pharmacy, medicine and life sciences, the physiological and pathological functions of H_2O_2 in biological systems will be better explained and understood. Hydrogen peroxide probes will have broader application prospects in the fields of pathophysiology, disease diagnosis and treatment.

Conflicts of interest

There are no conflicts to declare.

Acknowledgements

Notes and references

1 C. Nathan and A. Cunningham-Bussel, *Nat. Rev. Immunol.*, 2013, **13**, 349–361.

2 S. J. Dixon and B. R. Stockwell, *Nat. Chem. Biol.*, 2014, **10**, 9–17.

3 C. C. Winterbourn, *Nat. Chem. Biol.*, 2008, **4**, 278–286.

4 H. Wu, Q. Song, G. Ran, X. Lu and B. Xu, *TrAC, Trends Anal. Chem.*, 2011, **30**, 133–141.

5 F. L. Muller, M. S. Lustgarten, Y. Jang, A. Richardson and H. Van Remmen, *Free Radical Biol. Med.*, 2007, **43**, 477–503.

6 J. J. Hu, N. K. Wong, S. Ye, X. Chen, M. Y. Lu, A. Q. Zhao, Y. Guo, A. C. Ma, A. Y. Leung, J. Shen and D. Yang, *J. Am. Chem. Soc.*, 2015, **137**, 6837–6843.

7 A. A. Alfadda and R. Sallam, *J. Biomed. Biotechnol.*, 2012, **2012**, 936486.

8 T. F. Brewer, F. J. Garcia, C. S. Onak, K. S. Carroll and C. J. Chang, *Annu. Rev. Biochem.*, 2015, **84**, 765–790.

9 A. Kaur, M. A. Haghighatbin, C. F. Hogan and E. J. New, *Chem. Commun.*, 2015, **51**, 10510–10513.

10 L. A. Sena and N. S. Chandel, *Mol. Cell*, 2012, **48**, 158–167.

11 C. C. Winterbourn, *Biochim. Biophys. Acta*, 2014, **1840**, 730–738.

12 A. Gomes, E. Fernandes and J. L. F. C. Lima, *J. Biochem. Biophys. Methods*, 2005, **65**, 45–80.

13 P. D. Ray, B. W. Huang and Y. Tsuji, *Cell. Signalling*, 2012, **24**, 981–990.

14 N. Kumar, V. Bhalla and M. Kumar, *Coord. Chem. Rev.*, 2013, **257**, 2335–2347.

15 X. Sun, Q. Xu, G. Kim, S. E. Flower, J. P. Lowe, J. Yoon, J. S. Fossey, X. Qian, S. D. Bull and T. D. James, *Chem. Sci.*, 2014, **5**, 3368.

16 X. Zhou, Y. Kwon, G. Kim, J. H. Ryu and J. Yoon, *Biosens. Bioelectron.*, 2015, **64**, 285–291.

17 Z. Lou, P. Li and K. Han, *Acc. Chem. Res.*, 2015, **48**, 1358–1368.

18 K. Araki and K. Inaba, *Antioxid. Redox Signaling*, 2012, **16**, 790–799.

19 B. Chance, H. Sies and A. Boveris, *Physiol. Rev.*, 1979, **59**, 527–605.

20 H. C. Dawkes and S. E. Phillips, *Curr. Opin. Struct. Biol.*, 2001, **11**, 666–673.

21 J.-J. P. Kim and R. Miura, *Eur. J. Biochem.*, 2004, **271**, 483–493.

22 T. Finkel, *Curr. Opin. Cell Biol.*, 2003, **15**, 247–254.

23 J. R. Stone and S. Yang, *Antioxid. Redox Signaling*, 2006, **8**, 243–270.

24 P. Niethammer, C. Grabher, A. T. Look and T. J. Mitchison, *Nature*, 2009, **459**, 996–999.

25 C. Behl, J. B. Davis, F. Lesley and D. Schubert, *Cell*, 1994, **77**, 817–827.

26 B. D'Autreaux and M. B. Toledano, *Nat. Rev. Mol. Cell Biol.*, 2007, **8**, 813–824.

27 J. R. Stone and S. Yang, *Antioxid. Redox Signaling*, 2006, **8**, 243–270.

28 H. Ohshima, M. Tatemichi and T. Sawa, *Arch. Biochem. Biophys.*, 2003, **417**, 3–11.

29 K. J. Barnham, C. L. Masters and A. I. Bush, *Nat. Rev. Drug Discovery*, 2004, **3**, 205–214.

30 A. M. Shah and K. M. Channon, *Heart*, 2004, **90**, 485.

31 H. Rath and E. Schönpflug, *Bestimmung von Faserbegleitstoffen*, 1960.

32 R. Brandt and A. S. Keston, *Anal. Biochem.*, 1965, **11**, 6–9.

33 S. L. Hempel, G. R. Buettner, Y. Q. O'Malley, D. A. Wessels and D. M. Flaherty, *Free Radical Biol. Med.*, 1999, **27**, 146–159.

34 H. G. Kuivila and A. G. Armour, *J. Am. Chem. Soc.*, 1957, **79**, 5659–5662.

35 L. C. Lo and C. Y. Chu, *Chem. Commun.*, 2003, 2728.

36 M. C. Y. Chang, A. Pralle, E. Y. Isacoff and C. J. Chang, *J. Am. Chem. Soc.*, 2004, **126**, 15392–15393.

37 A. E. Albers, V. S. Okreglak and C. J. Chang, *J. Am. Chem. Soc.*, 2006, **128**, 9640–9641.

38 E. W. Miller, O. Tulyathan, E. Y. Isacoff and C. J. Chang, *Nat. Chem. Biol.*, 2007, **3**, 263–267.

39 B. C. Dickinson and C. J. Chang, *J. Am. Chem. Soc.*, 2008, **130**, 9638–9639.

40 A. E. Albers, B. C. Dickinson, E. W. Miller and C. J. Chang, *Bioorg. Med. Chem. Lett.*, 2008, **18**, 5948–5950.

41 C. Y. Ang, S. Y. Tan, S. Wu, Q. Qu, M. F. E. Wong, Z. Luo, P.-Z. Li, S. Tamil Selvan and Y. Zhao, *J. Mater. Chem. C*, 2016, **4**, 2761–2774.

42 J. Dong, Z. Zhao, R. Liu, H. Zhang, Y. Wu and X. Ba, *RSC Adv.*, 2017, 7, 55067–55073.

43 L. Du, M. Li, S. Zheng and B. Wang, *Tetrahedron Lett.*, 2008, **49**, 3045–3048.

44 L. Du, N. Ni, M. Li and B. Wang, *Tetrahedron Lett.*, 2010, **51**, 1152–1154.

45 J. Xu, Q. Li, Y. Yue, Y. Guo and S. Shao, *Biosens. Bioelectron.*, 2014, **56**, 58–63.

46 J. Xu, Y. Zhang, H. Yu, X. Gao and S. Shao, *Anal. Chem.*, 2016, **88**, 1455–1461.

47 Y. Liu, J. Niu, J. Nie, F. Meng and W. Lin, *New J. Chem.*, 2017, **41**, 3320–3325.

48 J. Han, C. Chu, G. Cao, W. Mao, S. Wang, Z. Zhao, M. Gao, H. Ye and X. Xu, *Bioorg. Chem.*, 2018, **81**, 362–366.

49 Y. Chen, X. Shi, Z. Lu, X. Wang and Z. Wang, *Anal. Chem.*, 2017, **89**, 5278–5284.

50 J. Liu, J. Ren, X. Bao, W. Gao, C. Wu and Y. Zhao, *Anal. Chem.*, 2016, **88**, 5865–5870.

51 J. Liu, S. Zhou, J. Ren, C. Wu and Y. Zhao, *Analyst*, 2017, **142**, 4522–4528.

52 W. Zhang, W. Liu, P. Li, F. Huang, H. Wang and B. Tang, *Anal. Chem.*, 2015, **87**, 9825–9828.

53 Z. Song, R. T. Kwok, D. Ding, H. Nie, J. W. Lam, B. Liu and B. Z. Tang, *Chem. Commun.*, 2016, **52**, 10076–10079.

54 J. Liu, C. Zhang, J. Dong, J. Zhu, C. Shen, G. Yang and X. Zhang, *New J. Chem.*, 2017, **41**, 4733–4737.

55 M. Ren, B. Deng, K. Zhou, X. Kong, J. Y. Wang and W. Lin, *Anal. Chem.*, 2017, **89**, 552–555.

56 X. Wang, Y. Huang, W. Lv, C. Li, W. Zeng, Y. Zhang and X. Feng, *Anal. Methods*, 2017, **9**, 1872–1875.

57 F. Dai, F. Jin, Y. Long, X. Jin and B. Zhou, *Free Radical Res.*, 2018, 1–151.

58 Z. Zhou, Y. Li, W. Su, B. Gu, H. Xu, C. Wu, P. Yin, H. Li and Y. Zhang, *Sens. Actuators, B*, 2019, **280**, 120–128.

59 L. Zhou, H. Ding, W. Zhao and S. Hu, *Spectrochim. Acta, Part A*, 2019, **206**, 529–534.

60 X. Liu, L. He, L. Yang, Y. Geng, L. Yang and X. Song, *Sens. Actuators, B*, 2018, **259**, 803–808.

61 X. Liu, H. Tian, L. Yang, Y. Su, M. Guo and X. Song, *Sens. Actuators, B*, 2018, **255**, 1160–1165.

62 J. Wang, W. Zhu, G. Niu, G. Jiang, Q. Chen, P. Gao, Y. Li, G. Zhang, X. Fan and B. Z. Tang, *Chem. Commun.*, 2018, **54**, 13957–13960.

63 F. Xu, W. Tang, S. Kang, J. Song and X. Duan, *Dyes Pigm.*, 2018, **153**, 61–66.

64 L. Yang, J. Y. Niu, R. Sun, Y. J. Xu and J. F. Ge, *Analyst*, 2018, **143**, 1813–1819.

65 N. Zhang, B. Dong, X. Kong, C. Wang, W. Song and W. Lin, *J. Fluoresc.*, 2018, **28**, 681–687.

66 X. Liang, X. Xu, D. Qiao, Z. Yin and L. Shang, *Chem. - Asian J.*, 2017, **12**, 3187–3194.

67 F. Xu, H. Li, Q. Yao, J. Fan, J. Wang and X. Peng, *J. Mater. Chem. B*, 2016, **4**, 7363–7367.

68 H. Xiao, P. Li, X. Hu, X. Shi, W. Zhang and B. Tang, *Chem. Sci.*, 2016, **7**, 6153–6159.

69 Y. Shen, F. Yan, X. Huang, X. Zhang, Y. Zhang, C. Zhang, J. Jin, H. Li and S. Yao, *RSC Adv.*, 2016, **6**, 88096–88103.

70 J. Shanmugapriya, K. Rajaguru, G. Sivaraman, S. Muthusubramanian and N. Bhuvanesh, *RSC Adv.*, 2016, **6**, 85838–85843.

71 C. Chung, D. Srikun, C. S. Lim, C. J. Chang and B. R. Cho, *Chem. Commun.*, 2011, **47**, 9618–9620.

72 M. Ren, B. Deng, J. Y. Wang, X. Kong, Z. R. Liu, K. Zhou, L. He and W. Lin, *Biosens. Bioelectron.*, 2016, **79**, 237–243.

73 Q. Ma, X. li, J. Zhang, X. Zhu, L. Zhou and H. Liu, *Anal. Methods*, 2017, **9**, 4558–4565.

74 H. Li, Q. Yao, J. Fan, J. Du, J. Wang and X. Peng, *Biosens. Bioelectron.*, 2017, **94**, 536–543.

75 G. Masanta, C. H. Heo, C. S. Lim, S. K. Bae, B. R. Cho and H. M. Kim, *Chem. Commun.*, 2012, **48**, 3518–3520.

76 C. S. Lim, M. K. Cho, M. Y. Park and H. M. Kim, *ChemistryOpen*, 2018, **7**, 53–56.

77 Y. Lu, X. Shi, W. Fan, C. A. Black, Z. Lu and C. Fan, *Spectrochim. Acta, Part A*, 2018, **190**, 353–359.

78 M. Kumar, N. Kumar, V. Bhalla, P. R. Sharma and Y. Qurishi, *Chem. Commun.*, 2012, **48**, 4719–4721.

79 D. Srikun, E. W. Miller, D. W. Domaille and C. J. Chang, *J. Am. Chem. Soc.*, 2008, **130**, 4596–4597.

80 G. Wu, F. Zeng, C. Yu, S. Wu and W. Li, *J. Mater. Chem. B*, 2014, **2**, 8528–8537.

81 S.-L. Zhong, J. Zhang, Q. Hu, W.-X. Chen, T.-F. Ma and J.-H. Zhao, *Asian Pac. J. Cancer Prev.*, 2014, **20**, 2254.

82 N. Velusamy, N. Thirumalaivasan, K. N. Bobba, A. Podder, S. P. Wu and S. Bhuniya, *J. Photochem. Photobiol., B*, 2018, **191**, 99–106.

83 L. He, X. Liu, Y. Zhang, L. Yang, Q. Fang, Y. Geng, W. Chen and X. Song, *Sens. Actuators, B*, 2018, **276**, 247–253.

84 L. Tang, M. Tian, H. Chen, X. Yan, K. Zhong and Y. Bian, *Dyes Pigm.*, 2018, **158**, 482–489.

85 J. Hou, M. Qian, H. Zhao, Y. Li, Y. Liao, G. Han, Z. Xu, F. Wang, Y. Song and Y. Liu, *Anal. Chim. Acta*, 2018, **1024**, 169–176.

86 K. Xu, L. He, X. Yang, Y. Yang and W. Lin, *Analyst*, 2018, **143**, 3555–3559.

87 Y. Shen, X. Zhang, Y. Zhang, Y. Wu, C. Zhang, Y. Chen, J. Jin and H. Li, *Sens. Actuators, B*, 2018, **255**, 42–48.

88 X. Lu, M. Zhao, P. Chen, Q. Fan, W. Wang and W. Huang, *J. Mater. Chem. B*, 2018, **6**, 4531–4538.

89 A. Sikora, J. Zielonka, M. Lopez, J. Joseph and B. Kalyanaraman, *Free Radical Biol. Med.*, 2009, **47**, 1401–1407.

90 J. Zielonka, A. Sikora, M. Hardy, J. Joseph, B. P. Dranka and B. Kalyanaraman, *Chem. Res. Toxicol.*, 2012, **25**, 1793–1799.

91 J. Zhou, Y. Li, J. Shen, Q. Li, R. Wang, Y. Xu and X. Qian, *RSC Adv.*, 2014, **4**, 51589–51592.

92 H. Maeda, Y. Fukuyasu, S. Yoshida, M. Fukuda, K. Saeki, H. Matsuno, Y. Yamauchi, K. Yoshida, K. Hirata and K. Miyamoto, *Angew. Chem., Int. Ed. Engl.*, 2004, **43**, 2389–2391.

93 K. Xu, B. Tang, H. Huang, G. Yang, Z. Chen, P. Li and L. An, *Chem. Commun.*, 2005, 5974–5976.

94 K. Xu, F. Liu, H. Wang, S. Wang, L. Wang and B. Tang, *Sci. China, Ser. B: Chem.*, 2009, **52**, 734–740.

95 J. Heo, C.-K. Lim, Y. Kim, H.-J. Cho, Y.-D. Lee, J.-h. Maeng, D.-R. Ahn, S. Lee, J. Bang, S. Y. Park and S. Kim, *Chem. Commun.*, 2016, **52**, 1131–1134.

96 H. Guo, G. Chen, M. Gao, R. Wang, Y. Liu and F. Yu, *Anal. Chem.*, 2019, **91**, 1203–1210.

97 Y. Sawaki and C. S. Foote, *J. Am. Chem. Soc.*, 1979, **101**(21), 6292–6296.

98 M. Abo, Y. Urano, K. Hanaoka, T. Terai, T. Komatsu and T. Nagano, *J. Am. Chem. Soc.*, 2011, **133**, 10629–10637.

99 M. Abo, R. Minakami, K. Miyano, M. Kamiya, T. Nagano, Y. Urano and H. Sumimoto, *Anal. Chem.*, 2014, **86**, 5983–5990.

100 B. Li, J.-B. Chen, Y. Xiong, X. Yang, C. Zhao and J. Sun, *Sens. Actuators, B*, 2018, **268**, 475–484.

101 M. S. Purdey, H. J. McLennan, M. L. Sutton-McDowall, D. W. Drumm, X. Zhang, P. K. Capon, S. Heng, J. G. Thompson and A. D. Abell, *Sens. Actuators, B*, 2018, **262**, 750–757.

102 C. Gao, Y. Tian, R. Zhang, J. Jing and X. Zhang, *Anal. Chem.*, 2017, **89**, 12945–12950.

103 X. Xie, X. Yang, T. Wu, Y. Li, M. Li, Q. Tan, X. Wang and B. Tang, *Anal. Chem.*, 2016, **88**, 8019–8025.

104 F. Yu, P. Li, P. Song, B. Wang, J. Zhao and K. Han, *Chem. Commun.*, 2012, **48**, 4980–4982.

105 S. I. Reja, M. Gupta, N. Gupta, V. Bhalla, P. Ohri, G. Kaur and M. Kumar, *Chem. Commun.*, 2017, **53**, 3701–3704.

106 N. Li, J. Huang, Q. Wang, Y. Gu and P. Wang, *Sens. Actuators, B*, 2018, **254**, 411–416.

107 Y. Hitomi, T. Takeyasu, T. Funabiki and M. Kodera, *Anal. Chem.*, 2011, **83**, 9213–9216.

108 Y. Hitomi, T. Takeyasu and M. Kodera, *Chem. Commun.*, 2013, **49**, 9929–9931.

109 D. Song, J. M. Lim, S. Cho, S.-J. Park, J. Cho, D. Kang, S. G. Rhee, Y. You and W. Nam, *Chem. Commun.*, 2012, **48**, 5449–5451.

110 Y. X. Liao, K. Li, M. Y. Wu, T. Wu and X. Q. Yu, *Org. Biomol. Chem.*, 2014, **12**, 3004–3008.

111 H. Guo, H. Aleyasin, B. C. Dickinson, R. E. Haskew-Layton and R. R. Ratan, *Cell & Bioscience*, 2014, **4**, 64.